Published by IOP Publishing for Sissa Medialab

Received: *January 20, 2020*
Accepted: *February 21, 2020*
Published: *March 30, 2020*

Plasma Physics by Laser and Applications (PPLA 2019)
Physics Department, University of Pisa, Pisa, Italy
29–31 October, 2019

2020 JINST 15 C03053

Biocompatible nanoparticles production by pulsed laser ablation in liquids

A. Torrisi,[a,1] **M. Cutroneo,**[a] **L. Torrisi**[b] **and J. Vacík**[a]

[a] *Nuclear Physics Institute of the Czech Academy of Sciences, Řež 25068, Czech Republic*

[b] *Dipartimento di Scienze Matematiche e Informatiche, Scienze Fisiche e Scienze della Terra (MIFT), Università di Messina, V.le F.S. d'Alcontres 31, S. Agata 98166, Messina, Italy*

E-mail: torrisi@ujf.cas.cz

Abstract: The preparation of spherical metallic nanoparticles (NPs), in the range of 10–100 nm, using pulsed laser ablation in water has particular interest in many scientific fields. The fast released laser energy to the solid metal in water produces plasma at the solid-liquid interface generating NPs in solution. The size distribution and the solution concentration depend by many parameters concerning the laser source (wavelength, pulse energy, pulse duration), the irradiation conditions (target depth in water, focal spot, repetition rate, irradiation time), and the medium where the ablation occurs (water, solution concentration, presence of surfactants). Optimal conditions can be found to control the average particle size, the size distribution, and the coalescence effect. A study of the NPs dependence from the ns pulsed Nd:YAG laser, irradiating metals in water is presented, discussing also the physical characterization of the produced NPs employing microscopy and optical analyses.

Keywords: Lasers; Plasma generation (laser-produced, RF, x ray-produced)

[1] Corresponding author.

https://doi.org/10.1088/1748-0221/15/03/C03053

Contents

1 **Introduction** 1

2 **Materials and methods** 1

3 **Experimental results** 3

4 **Discussions and conclusions** 8

1 Introduction

Pulsed laser ablation, consisting in the removing of atoms and molecules from an irradiated solid material, represents an optimal method to produce plasma [1, 2], to deposit thin films in vacuum [3], or to generate nano- and micro-particles in liquids [4, 5]. The main advantages of this method are represented by the simplicity and low cost and by the high purity of the obtained nanomaterials, which are not affected by chemical processes. Moreover, the laser parameters (wavelength, pulse duration, fluence), irradiation conditions (spot diameter, focal positioning with respect to the target surface, incident angle) and the target composition and geometry have a good control on the nanoparticles (NPs) production which action is fragmentedly reported in different articles. The NPs production in liquids represents an innovative technique to obtain high purity nanomaterials as colloid dispersions in solutions. Indeed, the NPs aggregation can be avoided by adding suitable surfactants to the solution [6]. Although different studies concerning the nanoparticle production were performed with the so-called "top-down" procedure, the too many parameters, controlling the particle size, shape and composition, may led to different results, depending on the experimental used setup, on the laser wavelength, pulse energy, pulse duration, laser repetition rate, ablated material and used liquid [7]. The aim of this paper is to present the results of some investigations concerning the dependence of the nanoparticle size generated in water by the laser parameters: fluence, irradiation time, wavelength and pulse duration. In particular the attention is devoted to Au, Ag and Ti-NPs, prepared in colloidal solutions, which are useful for many applications such as for filling porous materials [8], change the optical properties of polymers [9], control the electron density of laser-generated plasma [10] and, due to their high biocompatibility, are innovative for some biomedicine applications [11].

2 Materials and methods

The experimental setup consists of a high intensity pulsed laser and an optical system that focuses the laser beam on the surface of the target dipped in a liquid. The experiment was performed at the Laser Plasma Laboratory of the MIFT Department of the University of Messina with a Nd:YAG laser operating at the fundamental harmonic (1064 nm) with a pulse of 150 mJ energy, 3 ns duration and a repetition rate of 10 Hz. The laser beam is vertically deflected by a prism and is focused on the sample surface with 0.1–1 mm^2 spot surface by varying the focal distance with respect to the target surface. Au, Ag and Ti targets (as sheets with 1 cm^2 surface and 1 mm thickness) were irradiated

in distilled water (DW). The laser pulse, at an intensity of about 10^{10} W/cm^2, induces plasma at the solid target surface, which is confined by the overlying liquid. The plasma expansion produces a gas bubble generation, which expands and collapses quickly, cooling the plasma and generating atoms collisions and their aggregation in NPs [12]. The sample is placed in a polyethylene (PE) holder and covered by 5–20 mm water inside a glass tube. The holder allows small movements of the target due to the laser shock waves during the irradiation, which favors a uniform ablation of its surface. A different water volume in the glass tube affects the solution concentration and the NPs absorption of the laser light crossing the liquid. Generally, the metallic NPs are produced using 2.5 ml of distilled water and irradiation times ranging from 10 to 30 minutes to obtain solutions with different concentrations of NPs between 1 mg/ml to 10 mg/ml. In order to avoid or to reduce the effect of NPs coalescence, just after the laser irradiation was added a little quantity of surfactant sodium citrate (1 µg/ml) to the prepared solution. Figure 1a reports a scheme of the experimental apparatus and figure 1b shows a corresponding photo. Figure 1c, 1d [13] and 1e show the different colors of the solution obtained by irradiating Au in DW. The color is changing from transparent to pink and dark red with increasing the laser irradiation time, i.e., the gold nanoparticles (Au-NPs) concentration. TEM (Transmission electron microscope) images of NPs were obtained using a FEI Morgagni 268D microscope, equipped with a 1 k × 1 k SiS CCD camera Megaview II, and operating at the nominal accelerating voltage of 80 kV.

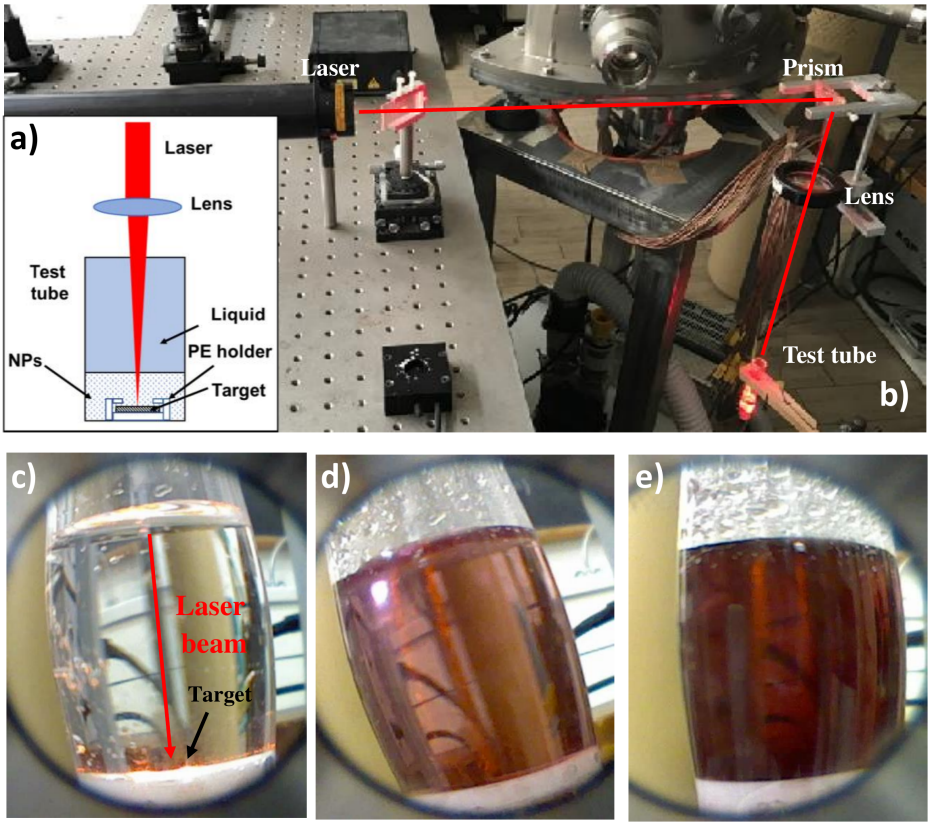

Figure 1. Scheme (a) and photo of the experimental apparatus for synthesis of the Au-NPs in water, inside a glass tube (b). The different colors of the solution are due to the different NPs concentrations, caused by increasing the laser irradiation time from transparent (c) to pink (d) and to dark red (e).

2020 JINST 15 C03053

Five microliters of the solution containing the NPs were pipetted onto a freshly glow-discharged Cu TEM grid covered with a thin layer of carbon, the excess of the applied solution was blotted by a Whatman #1 filter paper (GE Healthcare, Little Chalfont, U.K.), and the dried grid was finally inserted into the microscope. Images were acquired at the nominal magnification of 56 k×, yielding a pixel size of 1.1 nm. Absorbance measurements were performed at the Laboratory of the Messina University using a computerized monochromator (Horiba Jobin Yvon) with different lamps to cover the range 300–800 nm using a suitable cuvette in which the solution was contained for measurements of light transmission. In order to use sub-nanosecond laser pulses, NPs were also produced at the PALS laboratory in Prague (Czech Republic) using a Iodine laser operating at 1315 nm wavelength and 300 ps pulse duration, using a fluence of about 60 J/cm^2. Moreover, other NPs were produced at the IPPLM laboratory in Warsaw (Poland) using a titanium-sapphire laser operating at 800 nm wavelength, tens fs main laser pulse and a pre-pulse of about 20 ps duration.

3 Experimental results

The experiments were performed at the Physics of Laser Plasma Laboratory of MIFT, in Messina University (Italy) employing a 3 ns Nd:YAG laser operating at 1064 nm (fundamental), 532 nm (second harmonic) and 355 (third harmonic), with a maximum pulse energy of 800 mJ, operating in single mode or in repetition rate up to 10 Hz. The laser (spot size < 1 mm^2) hits solid targets placed in the bottom of a glass tube covered by distilled water (∼ 10 mm), as reported in figures 1a and 1b. The laser ablation in vacuum shows a different ablation yield in terms of ablated mass per laser pulse, growing with the laser fluence (J/cm^2), as reported in figure 2a. This plot shows that at the same value of laser fluence, the ablation yield decreases from Au to Ag and to Ti, mainly due to different thermal, electrical and optical properties of the investigated metals. Generally, metals with a lower boiling point and reflection coefficient and higher thermal end electrical conductivity increase the ablation yield, as occurs for gold with respect to titanium [14]. By the way, a high reflectivity reduces the laser energy absorbed in the target, inducing lower ablation yields. The photo thermal effects is enhanced in presence of high thermal and electric conductivity materials, due to the high thermal diffusion coefficient and diffusion length during the laser pulse duration, heating material far from the laser penetration volume and generating a major material evaporation. The laser ablation, in terms of removed mass per laser pulse, in fact, increases in high conductive metals with respect to insulators [15]. For example, the melting point, latent heat of vaporization, reflectance (at 1064 nm), thermal and electrical conductivity (at 20°C) for Au are 1064°C, 334 kJ/mol, 99%, 314 W/mK and 4.1×10^7 S/m, respectively, while for Ti are 1668°C, 421 kJ/mol, 58%, 20 W/mK and 2.4×10^6 S/m, respectively. Moreover, the ablation yields depend also by the surface roughness and contamination and by the environment conditions (target placed in vacuum, air or liquid). Figure 2b shows the different ablation yields in water as a function of the laser fluence for three different laser wavelengths, obtained using the fundamental, second and third Nd:YAG harmonics, corresponding to the 1064 nm, 532 nm and 355 nm wavelength, respectively. This last result was already presented and commented in [13].

It is possible to observe that in liquids the ablation yield decreases with respect to the vacuum, depending on the water depth at which the solid target is placed, in the glass tube. For instance, considering the Au target at 1064 nm and a fluence of 20 J/cm^2, the ablation yield in vacuum is

2020 JINST 15 C03053

0.9 μg/pulse, decreasing to 0.2 μg/pulse in water, using 10 mm liquid level on the target surface. The laser beam is multi-scattered in the solution containing the NPs. The solution concentration and the liquid thickness contribute both to increasing the laser absorption in the liquid, reducing the transmitted laser intensity reaching the solid target surface, and then the target ablation yield.

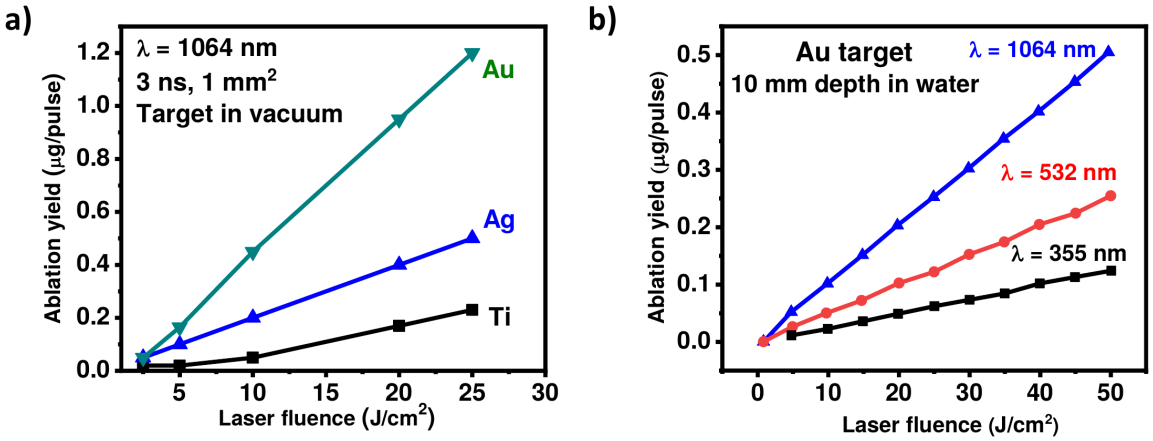

Figure 2. Ablation yield (μg/pulse) vs. laser fluence (J/cm^2), for different metallic targets (a) and for Au target irradiated at different laser wavelengths (b) [13].

The IR radiation depth is higher than ultraviolet (UV). It induces heating with a high ablation yield, while the UV radiation shows a high absorption coefficient, low penetration depth and generation of photochemical ablation. The visible radiation has an intermediate behaviour between IR and UV. It is possible to observe a decreasing in the ablation yield of Au in water with respect to the ablation in vacuum. This effect is due mainly to the partial laser absorption and scattering in the overlaying water above the solid target. The NPs produced in the liquid have a size within a restricted range of values (from 10 to 100 nm), measurable by TEM. An example referred to Au-NPs generated in DW at 1064 nm wavelength, 150 mJ energy and 3 ns pulse duration, is reported in figure 3a and in the zoom of figure 3b. In this case, the size ranges within 2 and 15 nm with an average value of 10 nm. Another important aspect of the produced NPs concerns their surface optical properties. In particular, measurements of UV-Visible absorbance versus wavelength, obtained with a suitable spectrophotometer and performed at MIFT of Messina University demonstrated that an absorption peak is centred at about 520 nm wavelength. This peak depends on the NPs diameter which shifts towards higher wavelengths increasing its size. This is due to the Surface Plasmon Resonance (SPR) absorption effects [16]. It suggests that NPs have high resonant absorbance in correspondence of a specific wavelength band, at which value the incident light induces an electric dipole on the NPs surface and the electrons oscillating at the plasma resonant frequency enhance the effect of light absorption. A typical absorbance spectrum vs. wavelength is reported in figure 3c for Au-NPs, showing the SPR effect at about 523 nm wavelength. The SPR absorbance peak increases for high concentrations of Au-NPs in water, and the band enlarges for large size distributions. Increasing the Au-NPs, the peak shifts towards higher wavelengths. This effect happens also in presence of the NPs aggregation. A typical Au-NPs distribution produced in DW is reported in figure 3d for an average Au diameter of 15 nm with a spread size of about ± 5 nm (FWHM).

2020 JINST 15 C03053

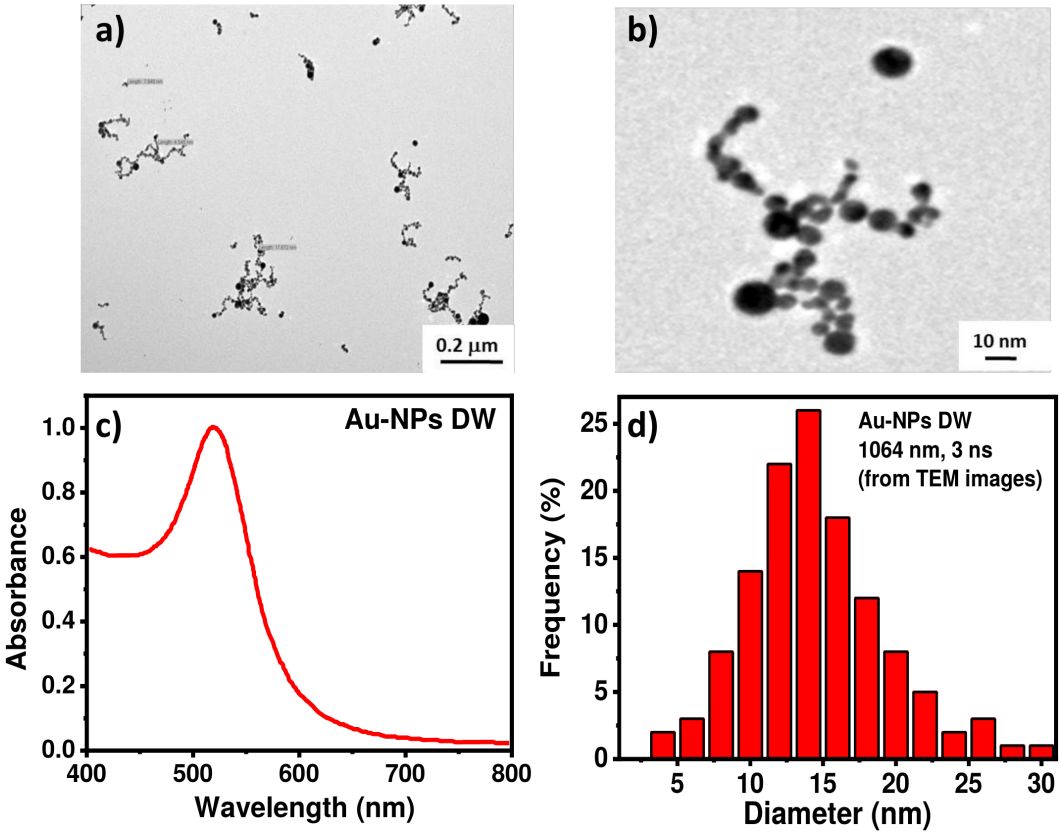

Figure 3. TEM image of Au-NPs generated in distilled water (DW) at low (a) and high magnification (b), absorbance of the solution as a function of the wavelength (c), and diameter distribution of the produced nanoparticles (d).

The nanoparticle size generally decreases with the laser fluence up to a limit after which stabilize. Various causes may generate this effect, such as the self-absorption of the laser light in the colloidal NPs solution, their partial fragmentation induced by the laser light crossing the solution, as well as the laser pulse energy reduction arriving on the solid metallic target crossing the liquid level. The laser light, in fact, is absorbed by the NPs in the produced solution especially at high solution concentration. This energy absorption can be sufficient to produce fragmentation with nanoparticle size reduction. The laser light in the high concentrated solution is also scattered and the transmitted component to the target decreases significantly at a low intensity. Figure 4a shows a typical trend for the Au-NPs size in DW as a function of the laser fluence ranging from 1 up to 70 J/cm^2. The use of the repetitive laser shots at 10 Hz frequency repetition rate produces not only laser ablation of the target immersed in the water, but also the fragmentation of the produced colloidal NPs dispersed in the solution. As for gold, generally the average NPs size decreases with the laser fluence because high energy produces higher vaporization. However, the solution concentration, at 10 Hz repetition rate, rapidly enhances and absorbs more laser energy, inducing NPs fragmentation in the liquid and transmitting less laser pulse energy to the metallic target.

Thus, less vapour generates smaller NPs. At high fluence the smaller NPs are produced in the liquid solution and in the solid target. This phenomenon induces a decrement of the nanoparticle size up to a final stabilization, after about 10 min irradiation time, as reported in the plot of figure 4b,

referred to Au irradiated at 1064 nm with a fluence of 10 J/cm^2 [17]. The comparison between the data reported in figure 4a and 4b shows that it is possible to obtain different NPs size at the same fluence, even if the laser pulse and the water level on the target surface are different. Indeed, in figure 4a the average size is lower with respect to the data reported in figure 4b, because the laser energy is lower and the water level, absorbing the laser energy, is higher. For example, at 10 min irradiation time figure 4a reports that using 60 mJ and 15 mm water depth the size is 10 nm at 10 J/cm^2, while figure 4b reports that at 10 min irradiation time, 100 mJ pulse energy and 8 mm water depth (level) the size is about 27 nm. This result is due to the higher laser intensity arriving at the target when 8 mm water thickness is employed. The laser wavelength influences the penetration depth in the target and the ablation yield, as reported in figure 2b. It influences also the nanoparticle average size, producing larger particles using IR radiation, and smaller size particles using UV radiation. Typical measurements are shown in figure 5a for Ag-NPs produced with an average value of 14 nm, 18 nm and 10 nm employing a Nd:YAG laser operating at the 1064, 532 and 355 nm wavelength, respectively. The optical absorbance measurements on these different NPs suspended in water are reported in figure 5b for the different nanoparticle size obtained at the same irradiation times.

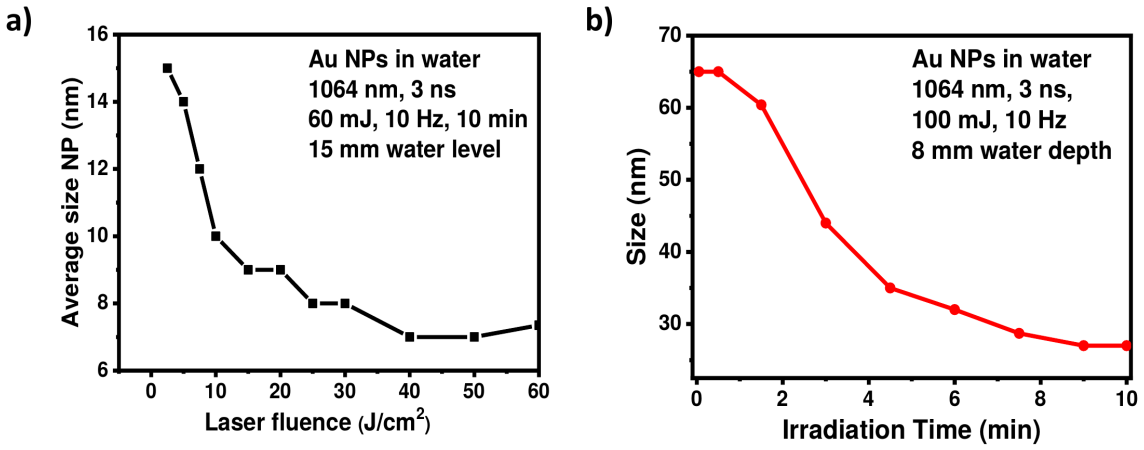

Figure 4. Average size of the Au-NPs in water as a function of the laser fluence (a), and of the irradiation time in repetition rate at 10 Hz (b).

The data presented in figure 5 for Ag-NPs are similar for Au and Ti NPs. It is evident that the number of NPs produced by IR radiation, as well as their size, is higher with respect to that produced using UV radiation [13]. In fact, not only the yield increases inducing photo-thermal effects, but also a little SPR shift occurs towards the higher wavelengths for NPs produced by IR with respect to UV radiations. An important aspect concerning the NPs in liquids is represented by their possible aggregation and coalescence induced by Van der Waals and electrical forces.

The coalescence generally increases with the time and with the temperature producing micrometric particles and precipitates in the solution. The presence of coalescence and formation of bigger NPs aggregations shifts the absorbance SPR spectrum towards the higher wavelengths, as reported in figure 6a for Au-NPs. In order to avoid these effects, surfactants at low concentration can be added to the solution, e.g., a little amount of sodium citrate. The ionic surfactant molecules, carrying a net electrical charge, are deposited on the NPs, covering their surface (cupping effect), and consequently inducing electrical repulsion between the NPs [18].

2020 JINST 15 C03053

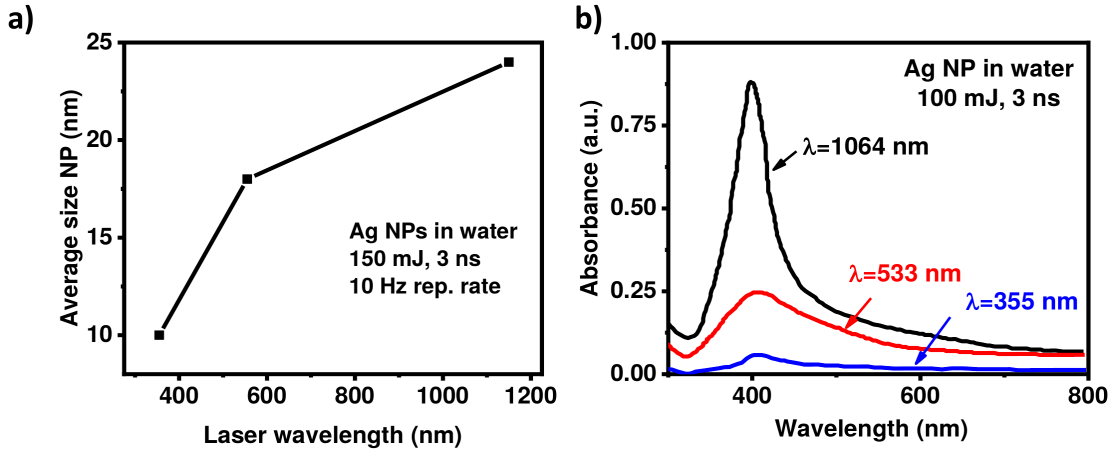

Figure 5. Average size of Ag-NPs in water as a function of the laser wavelength (a), and absorbance as a function of the light wavelength and of the laser ablation wavelength (b).

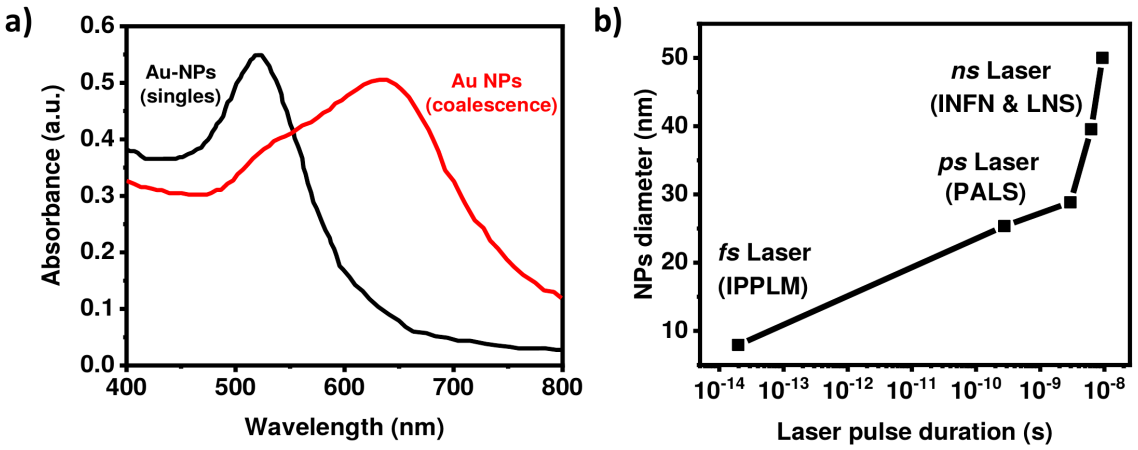

Figure 6. Comparison of absorbance of the Au-NPs colloidal dispersion in water in presence of single nanoparticles and Au-NPs coalescence (a), and Ag-NPs diameter as a function of the laser pulse duration (b).

Finally, the nanoparticle size depends also on the laser pulse duration, and in general, it increases in diameter with the pulse duration as a result of the higher thermal effect and higher collision time of the atoms inside the plasma expansion forming the bubble gas at the solid-liquid interface. In order to investigate on the effects of different laser pulse duration, specific measurements were performed irradiating Au-NPs in water employing lasers operating from 40 fs up to 9 ns. The minimum pulse duration was obtained using the 40 fs Ti:sapphire laser, 800 nm wavelength and single pulse, at the Institute of Plasma Physics and Laser Microfusion (IPPLM, Warsaw, Poland). The middle pulse duration was obtained using the 300 ps Asterix laser operating at 1350 nm wavelength in single mode at PALS laboratory in Prague, Czech Republic. The lasers operating at 3 ns and 6 ns were the Nd:YAG lasers of the MIFT Department of Messina University (Messina, Italy). The laser operating at 9 ns was a Nd:YAG laser operating at INFN-Laboratori Nazionali del Sud in Catania, Italy. The experimental setups used for these experiments were similar to that reported in figure 1. In the IPPLM and PALS laboratories a splitter was employed to extract a part of the laser beam in air

2020 JINST 15 C03053

and to focus it on the target placed in water inside the glass tube. Nanoparticle sintering performed with different lasers in similar conditions of wavelength and fluence, pointed at an increment of the Au-NPs average size from 25 nm up to 50 nm using sub-ps, ps and ns lasers, respectively, in agreement with the literature [19] (figure 6b). Such measurements were followed by SEM and TEM microscopy characterizations.

4 Discussions and conclusions

In this work, an investigation concerning the laser production of the metallic NPs is presented and discussed, with a special attention to the dependence of the NPs size on the laser parameters. The presented results better describe the influence of the laser fluence, irradiation time, laser wavelength and laser pulse duration on the NPs size and ablation yield, providing useful information in a growing scientific field of interest which is developing more than the chemical synthesis of nanoparticles. The experimental setup is simplified in order to realize the experiment with a laptop laser. The method of nanoparticle preparation is cheap and accurate, permitting to synthetize pure NPs without addition of chemical reagents (they are used in the "bottom-up" method in chemical reactions to fabricate the NPs). The NPs size depends on many factors, such as the laser fluence, which decreases the average size, and the repetition rate, which results in NPs fragmentation. The total irradiation time can also influence the average size. Indeed, the NPs size decreases with prolonged irradiations, inducing their fragmentation. The laser wavelength also influences the NPs size, enhancing the size by IR radiations and reducing the size with UV radiations. The laser pulse duration plays an important role as well, enabling the generation of the higher sized NPs using the ns laser pulses, instead than the ps or fs laser pulses. The accurate preparation of the metallic NPs permits to apply them in several physical applications, as well as in chemistry, engineering, microelectronics and biomedicine. In physics, for example, they are permitting to modify the properties of many materials, such as NPs embedded in polymers change the optical absorbance and electrical conductivity of the polymeric matrix, permitting their laser welding, the realization of conductive tracks and the control of the electron density in the laser-generated plasmas [20]. In chemistry, they are functionalized with particular molecules that then act as catalysers in specific chemical reactions. In engineering, they can be used to modify the mechanical properties of many materials, such as graphene, polymers and ceramics. In microelectronics, they are employed to change the electrical and optical properties of electronic devices, sensors and photovoltaic cells [21]. In biomedicine, they found many applications, e.g., as particles changing the wetting ability and viscosity of fluids, contrast media for diagnostic imaging, or material for hyperthermia and radiotherapy applications using visible or ionizing radiations in order to deposit high doses to the tumour tissues and cells where the NPs are injected [22]. Future developing in this area concerns the possibility to realize not only metallic nanoparticles but also insulator, semiconductive and polymeric nanoparticles, and not only spherical but also different geometry. Moreover, the laser production can be thermally assisted and in presence of reactive gases can generate nanocrystals and nanostructures with special properties. Moreover, functionalized and biocompatible NPs can be realized to be employed in biomedicine [23, 24].

2020 JINST 15 C03053

Acknowledgments

This work was supported in part by the by the Research & Mobility project of Messina University No. 74893496, scientifically coordinated by Professor L. Torrisi and in part by Grant Agency for the Czech Republic, project GACR No. 18-07619S.

References

[1] L. Torrisi et al., *LAMQS and XRF analyses of ancient Egyptian bronze coins*, *Radiat. Eff. Defects Solids* **165** (2010) 626.

[2] A. Torrisi, P.W. Wachulak, H. Fiedorowicz and L. Torrisi, *Monitoring of the plasma generated by a gas-puff target source*, *Phys. Rev. Accel. Beams* **22** (2019) 052901.

[3] T.W. Reenaas et al., *Femtosecond and nanosecond pulsed laser deposition of silicon and germanium*, *Appl. Surf. Sci.* **354** (2015) 206.

[4] L. Torrisi, *Micron-size particle emission from bioceramics induced by pulsed laser deposition*, *Bio-Med. Mater. Eng.* **3** (1993) 43.

[5] L. Torrisi and C. Scolaro, *Nanoparticles improving the wetting ability of biological liquids*, *J. Thermodyn. Catal.* **08** (2017) 1.

[6] P. Kazakevich, A. Simakin, V. Voronov and G. Shafeev, *Laser induced synthesis of nanoparticles in liquids*, *Appl. Surf. Sci.* **252** (2006) 4373.

[7] V. Amendola and M. Meneghetti, *What controls the composition and the structure of nanomaterials generated by laser ablation in liquid solution?*, *Phys. Chem. Chem. Phys.* **15** (2013) 3027.

[8] R.W. Murray, *Nanoelectrochemistry: Metal nanoparticles, nanoelectrodes, and nanopores*, *Chem. Rev.* **108** (2008) 2688.

[9] L. Torrisi, F. Caridi, A. Visco and N. Campo, *Polyethylene welding by pulsed visible laser irradiation*, *Appl. Surf. Sci.* **257** (2011) 2567.

[10] L. Torrisi, G. Ceccio and M. Cutroneo, *Laser-generated plasma by carbon nanoparticles embedded into polyethylene*, *Nucl. Instrum. Meth.* **B 375** (2016) 93.

[11] L. Torrisi et al., *Laser-produced au nanoparticles as X-ray contrast agents for diagnostic imaging*, *Gold Bull.* **50** (2017) 51.

[12] N. Restuccia and L. Torrisi, *Nanoparticles generated by laser in liquids as contrast medium and radiotherapy intensifiers*, *EPJ Web Conf.* **167** (2018) 04007.

[13] L. Torrisi and A. Torrisi, *Laser ablation parameters influencing gold nanoparticle synthesis in water*, *Radiat. Eff. Defects Solids* **173** (2018) 729.

[14] M. Jiang, X. Wu, Y. Wei, G. Wilde and L. Dai, *Cavitation bubble dynamics during pulsed laser ablation of a metallic glass in water*, *Extreme Mech. Lett.* **11** (2017) 24.

[15] L. Torrisi, A. Borrielli and D. Margarone, *Study on the ablation threshold induced by pulsed lasers at different wavelengths*, *Nucl. Instrum. Meth.* **B 255** (2007) 373.

[16] M.A. Garcia, *Surface plasmons in metallic nanoparticles: fundamentals and applications*, *J. Phys.* **D 45** (2012) 389501.

[17] L. Torrisi et al., *Gold nanoparticles produced by laser ablation in water and in graphene oxide suspension*, *Philos. Mag.* **98** (2018) 2205.

2020 JINST 15 C03053

[18] T. Sakai, H. Enomoto, K. Torigoe, H. Sakai and M. Abe, *Surfactant- and reducer-free synthesis of gold nanoparticles in aqueous solutions*, *Colloids Surf.* **A 347** (2009) 18.

[19] T. Kim, K. Lee, M.-s. Gong and S.-W. Joo, *Control of gold nanoparticle aggregates by manipulation of interparticle interaction*, *Langmuir* **21** (2005) 9524.

[20] L. Torrisi, M. Cutroneo and G. Ceccio, *Effect of metallic nanoparticles in thin foils for laser ion acceleration*, *Phys. Scripta* **90** (2014) 015603.

[21] T. Pfeiffer et al., *Plasmonic nanoparticle films for solar cell applications fabricated by size-selective aerosol deposition*, *Energy Procedia* **60** (2014) 3.

[22] L. Torrisi, N. Restuccia and I. Paterniti, *Gold nanoparticles by laser ablation for X-ray imaging and protontherapy improvements*, *Recent Pat. Nanotechnol.* **12** (2018) 59.

[23] T. Shinonaga, S. Kinoshita, Y. Okamoto, M. Tsukamoto and A. Okada, *Formation of periodic nanostructures with femtosecond laser for creation of new functional biomaterials*, *Procedia CIRP* **42** (2016) 57.

[24] G. Yang, *Laser ablation in liquids: Applications in the synthesis of nanocrystals*, *Prog. Mater Sci.* **52** (2007) 648.

2020 JINST 15 C03053